



**HAL**  
open science

## The variegated scallop, *Mimachlamys varia*, undergoes alterations in several of its metabolic pathways under short-term zinc exposure

P. Ory, V. Hamani, P.-E. Bodet, Laurence Murillo, M. Graber

### ► To cite this version:

P. Ory, V. Hamani, P.-E. Bodet, Laurence Murillo, M. Graber. The variegated scallop, *Mimachlamys varia*, undergoes alterations in several of its metabolic pathways under short-term zinc exposure. *Comparative Biochemistry and Physiology - Part D: Genomics and Proteomics*, 2021, 37, pp.100779. 10.1016/j.cbd.2020.100779 . hal-03137735

**HAL Id: hal-03137735**

**<https://hal.science/hal-03137735v1>**

Submitted on 10 Feb 2021

**HAL** is a multi-disciplinary open access archive for the deposit and dissemination of scientific research documents, whether they are published or not. The documents may come from teaching and research institutions in France or abroad, or from public or private research centers.

L'archive ouverte pluridisciplinaire **HAL**, est destinée au dépôt et à la diffusion de documents scientifiques de niveau recherche, publiés ou non, émanant des établissements d'enseignement et de recherche français ou étrangers, des laboratoires publics ou privés.

1 **The variegated scallop, *Mimachlamys varia*, undergoes alterations in several of its metabolic**  
2 **pathways under short-term zinc exposure**

3 P. Ory<sup>1</sup>, V. Hamani<sup>1</sup>, P.-E. Bodet<sup>1</sup>, L. Murillo<sup>1</sup>, M. Graber<sup>1\*</sup>

4 <sup>1</sup>Littoral Environnement et Sociétés (LIENSs), UMR 7266, CNRS-Université de La Rochelle, 2 rue Olympe  
5 de Gouges, F-17042 La Rochelle Cedex 01, France.

6  
7 **Abstract**

8 The variegated scallop (*Mimachlamys varia*) is a filter feeder bivalve encountered in marine regions of the  
9 Atlantic coast. In particular, it is present in the La Rochelle marina (France), where it is used for the  
10 biomonitoring of marine pollution, due to its ability to strongly bioaccumulate pollutants. In this semi-closed  
11 environment, contamination generated by port activities leads to an accumulation of both organic and metal  
12 pollutants. Zinc is one of these pollutants, present at a dose of up to 150 to  $\mu\text{g}\cdot\text{L}^{-1}$ . This study investigated the  
13 effects of 48 h zinc exposure upon the metabolic profiles of *Mimachlamys varia* using UHPLC/QToF (ultra-  
14 high performance liquid chromatography-quadrupole time-of-flight) tandem mass spectrometry  
15 metabolomics. After acclimation in mesocosms recreating *in situ* conditions, both controls and exposed with  
16  $\text{Zn}^{2+}$  (150  $\mu\text{g}\cdot\text{L}^{-1}$ ) bivalves were dissected to recover the gills after 48 h and stored at  $-80^{\circ}\text{C}$  before  
17 metabolites extraction. UHPLC/QToF tandem mass spectrometry was performed to study metabolite  
18 composition of samples. Statistical analysis of results using multivariate techniques showed a good  
19 classification between control and exposed groups. Eleven identified metabolites were found to be down-  
20 modulated in exposed scallops. These variations could reflect potential zinc effects on several of the  
21 biological processes, such as energy metabolism, osmoregulation and defense against oxidative stress.  
22 Among the eleven metabolites highlighted, four were reported for the first time in an aquatic organism  
23 exposed to Zn. This study demonstrates once again the diversity of interactions between bivalves and metals  
24 and the complexity of the physiological response of marine bivalves to pollutants.

25  
26 **Keywords:** Zinc, UHPLC/QToF mass spectrometry, metabolomics, *Mimachlamys varia*.

27 \*Corresponding author at : Marianne Graber, Littoral Environnement et Sociétés (LIENSs), UMR 7266,  
28 CNRS-Université de La Rochelle, 2 rue Olympe de Gouges, F-17042 La Rochelle Cedex 01, France. Email  
29 adress : mgraber@univ-lr.fr

30

31

32

### 33 **Introduction**

34 Marine ecosystems are the final receptacle of contaminants released to the environment, especially in  
35 seaports and other industrialized or strongly anthropised coastal areas. Boat harbours, for instance, may be  
36 hotspots of contaminant accumulation (Bighiu et al., 2017; Johnston et al., 2011). Indeed, they are likely to  
37 receive both a cumulative load of pollutants from upstream point and nonpoint sources from watershed, and  
38 many pollutants generated at the marina itself. In addition, the construction of a marina generally creates a  
39 condition of reduced water circulation and protection from wave action. The result is an area with limited  
40 natural water circulation and exchange. The marina of La Rochelle, located in the south-west of France,  
41 perfectly illustrates this phenomenon with its complex geometry and infrastructure, especially since its  
42 expansion in 2014 (Huguet et al., 2019). Over time, this reduced circulation and increased pollutant  
43 generation can increase pollutant concentrations in the water column, sediments, and aquatic organisms. This  
44 often results in greater impacts in the area concerned on ecological communities (Sim et al., 2015). Because  
45 of their environmental persistence, heavy metals are one of the major harmful toxic pollutants for the marine  
46 environment (Stankovic et al., 2014) and especially in harbours and marina (Bighiu et al., 2017; Galkus et  
47 al., 2012). The major proportion of these trace elements is trapped in coastal sediments where they can be  
48 continuously released into the water column and incorporated into food webs. The availability of trace  
49 elements to aquatic species is of prime concern both in terms of the prediction of the effects of metal  
50 pollution on ecosystems and in terms of public health when bioaccumulated in edible animals.

51 In the following study, we focused attention on Zn pollution, at a concentration such as the maximum  
52 concentration that can be reached in the marina of La Rochelle. Zinc is found at  $157 \mu\text{g}\cdot\text{L}^{-1}$  in the water of  
53 the Marillac area, which is one of the four docks that make up the marina of les Minimes (CREOCEAN,  
54 2018). It may arise from nonpoint sources from watershed : rainwater runoff sources (outdoor zinc or  
55 galvanised surfaces, tire wear debris, etc.), zinc-containing paints, anti-corrosion additives for water-  
56 containing equipment, fireworks, motor oil/lubricating oils additives, industrial air emissions, industrial  
57 runoff, zinc minerals or wastes in construction materials, fertiliser and agricultural micronutrient products  
58 (California Stormwater Quality Association [CASQA] 2015). It also has its origin in the boat components  
59 and their maintenance: zinc anodes used to deter corrosion of metal hulls and engine parts, zinc constituent  
60 of motor oil and tires, antifouling paints (Eklund and Eklund, 2014).

61 Among the marine organisms most affected by metal pollution are bivalve mollusks, given their filter-  
62 feeding attitude, which leads to a strong accumulation of the pollutants. In order to investigate the unknown  
63 toxicological effects and mechanisms of metals on bivalves, environmental metabolomics is commonly  
64 applied for several years now (for reviews see: Booth et al., 2011, Viant and Sommer, 2012, Lankadurai et  
65 al., 2013). As examples of recent metabolomics application in the case of a metal contamination of bivalves,  
66 Aru et al. (2016) investigated the effects of short-term lead and zinc exposure upon the metabolic profiles of  
67 clams *Ruditapes decussatus* and *Ruditapes philippinarum*. Nguyen et al. (2018) applied an integrated  
68 approach that combines flow cytometry and metabolomics to characterize cellular and molecular

69 mechanisms of copper immunotoxicity in mussel (*Perna canaliculus*). Wu et al. (2017) found that mussel  
70 response to cadmium was dependent on life cycle stage. Many other current applications of  
71 metabolomics to study the effects of metals or other water contaminants on marine organisms have been  
72 reported in many studies (for a review see Pomfret et al., 2019).

73 Here, we used the marine bivalve *Mimachlamys varia*, in the family *Pectinidae*, commonly known as the  
74 variegated scallop, as a model organism. Due to its relative abundance along the Atlantic coasts, its  
75 sedentary nature and also because this species has been shown to have a very elevated pollutants  
76 incorporation and retention capacity, it has been proposed as a potential indicator species for the marine  
77 biomonitoring (Breitwieser et al., 2018a; Metian et al., 2009a, 2009b; Milinkovitch et al., 2015). In  
78 particular, it is relatively easy to sample in the marina of La Rochelle, where it has been used for  
79 ecotoxicological studies (Breitwieser et al., 2018b). Furthermore, it is a commercially harvested species also  
80 captured for leisure activities, directly on the shore or by snorkeling and it represents therefore a definite  
81 economic value.

82 Previously, we performed a first metabolomics study on *M. varia* that highlighted a complex metabolic  
83 reprogramming that occurs during tidal cycles after an emersion period of 2 h and upon re-immersion (Ory et  
84 al., 2019). It appeared that metabolites depend on the moment of the tidal cycle as well as on the ambient  
85 environment (oxygenation, salinity and temperature conditions, seasonality, etc.). In order to minimise the  
86 effects of all these important interplaying environmental factors and understand the underlying mechanisms  
87 affecting *M. varia* exposed to zinc, we grew scallops in aquaria under controlled and continuously immersed  
88 conditions and we exposed the animals to zinc concentration equal to that found in La Rochelle marina. A  
89 comparative metabolomics study was performed in gills samples, using UHPLC/QToF mass spectrometry, in  
90 order to provide an overview of the relationship between zinc exposure and metabolome changes. Gills were  
91 preferred over other tissues, as they have been shown to be, along with the mantle and digestive gland, the  
92 main storage organs for metals in oysters (Wang et al., 2018). In addition, gills are generally considered as  
93 the main entry of dissolved metals in marine filter-feeder organisms (Marigómez et al., 2002).

94

## 95 **Materials and Methods**

96

### 97 *Animals and experimental design*

98 Scallops, *Mimachlamys varia*, (shell length from 3 to 5 cm) were collected from La Pointe du Grouin to Loix  
99 en Ré (Ré island, France) and acclimated one month in the laboratory in filtered through a 50 µm nylon filter  
100 and sterilised seawater. The physicochemical parameters of the water were controlled every two days and  
101 were kept constant by a biweekly water renewal (pH 8.0, temperature 10°C, salinity 33 g.kg<sup>-1</sup> seawater,  
102 nitrite, nitrate, and ammonia <0.025 mg.L<sup>-1</sup>). Food as liquid algal culture (Shellfish Diet 1800®, Reed  
103 Mariculture, Campbell, CA, USA) was distributed three times per week, at a rate of 0.02 mL per individual.  
104 Mortality of less than 3% was observed in acclimation tanks.

105 For this experiment, 36 scallops were randomly distributed in six 18-litres aquaria. Three randomly selected  
106 aquaria were contaminated with a ZnCl<sub>2</sub> solution (nominal zinc concentration 150 µg.L<sup>-1</sup>). The other three  
107 aquaria received the same amount of seawater.

108 After 48 hours of exposure, the six scallops remaining in each aquarium were sampled. The gill tissues of  
109 each individual were dissected, drained on absorbent paper and put in cryovial on ice. Gill tissues from three  
110 individuals were grouped, snap-frozen in liquid nitrogen and stored in a freezer at -80°C. From this  
111 sampling, six exposed samples and six controls were obtained. These control samples were used as a  
112 reference for the analyses.

113

#### 114 *Sample preparation for metabolomics study*

115 Sample preparation was performed according to a previously described method (Ory et al., 2019), inspired  
116 by a metabolomics study in Phycotoxines laboratory (Ifremer, Nantes, France) (Mondeguer et al., 2015). In  
117 summary, samples were thawed, homogenized by manual grinding and then crushed with a homogenizer.  
118 These three last operations were performed on ice. They were then adjusted to 1 g and stored at -80°C before  
119 extraction procedure. This last protocol included a triple solvent extraction by successively using acetone  
120 twice and methanol. The three pooled supernatants were recovered and dried with a stream of nitrogen,  
121 before resuspension with 2 mL methanol/water 20/80 (v/v), storage at -80°C, filtration with 0.2 µm filters  
122 and LC/MS analysis.

123

#### 124 *UHPLC/QToF MS analysis of metabolites*

125 The analysis of metabolites in gills was performed by ultra-high-performance liquid chromatography  
126 coupled to high resolution mass spectrometry, according to a previously described method (Ory et al., 2019),  
127 with the same analytical equipment. 5 µL of the samples were injected in a column “Acquity UPLC HSST3”  
128 (Waters) (2.1 × 150 mm, 1.7 µm), and the products were eluted at a flow rate of 300 µL.min<sup>-1</sup> using a  
129 gradient composed of solvents A (water/formic acid 100/0.001 (v/v)) and B (acetonitrile/ formic acid  
130 100/0.001 (v/v)). The gradient used was the same as described previously (Ory et al., 2019). The analyses  
131 were performed in positive and negative ionisation mode with MS<sup>E</sup> function in a centroid mode. The MS  
132 parameters applied in the ESI source for the two ionisation modes were the same as described previously  
133 (Ory et al., 2019), except that desolvation gas flow-rate was 300 L.h<sup>-1</sup> and capillary voltage was 3 kV (+) and  
134 2.5 kV (-) and sampling cone 35 V. The instrument was adjusted for the acquisition on a 50–2100 m/z  
135 interval, with a scan time of 0.5 s. A 20 to 40 V ramp was used as collision energy for the high energy mode  
136 of MS<sup>E</sup>.

137 The mass spectrometer was calibrated before analysis using 0.5 mM sodium formiate solution and the  
138 Leucine Enkephalin (M = 555.62 Da, 1 ng.µL<sup>-1</sup>) was used as a lock-mass.

139 Compound identification was performed as explained below.

140

141

142 *Quality Control*

143 A pool sample was prepared by combining 100 µL of each gills tissue extract. This mixture was divided into  
144 ten vials that were used as quality-control samples (QCs). They were regularly distributed and injected  
145 throughout the sample list to ensure analytical repeatability. Samples of gill tissue extracts were measured in  
146 randomised order. Blanks were prepared with the last extraction solvent and injected at the beginning and at  
147 the end of the sample sequence, to allow the subsequent subtraction of contaminants or components coming  
148 from the extraction solvent.

149  
150 *Chemicals*

151 Acetonitrile, Methanol, Acetone with HPLC grade purity were from Carlo Erba. Water was prepared using a  
152 Milli-Q reagent water system. Succinate and L-phenylalanine were purchased from Sigma-Aldrich (now part  
153 of Merck).

154  
155 *Statistical analysis*

156 Metabolites data were obtained and treated as ion peak intensity as previously described (Ory et al., 2019).  
157 Data were processed on the online and freely available Workflow4Metabolomics (W4M) platform  
158 (<http://workflow4metabolomics.org>) for pretreatments and multivariate analyses processing as previously  
159 described (Ory et al., 2019). Pretreatments included batch correction and removing metabolites with  
160 coefficients of variation (CV) > 0.4 in the QC samples. Quality metrics tool (supplied by W4M Core  
161 Development Team) provided visualising the data matrices, batch correction efficiency and supplied a rapid  
162 highlight of potential sample outliers.  
163 Log-transformation normalised the data and Pareto scaling was applied before the multivariate analysis  
164 process. The data were analysed with unsupervised (Principal Component Analysis, PCA) and supervised  
165 (Partial Least Square Discriminant Analysis, PLS-DA) methods. This last method is a multivariate regression  
166 and prediction based on the separation between two classes: reference and Zn-exposed samples after a 48 h  
167 exposure. It allowed the selection of metabolites involved in class separation in order to identify metabolites  
168 affected by Zn exposure. Metabolites responsible for classification between groups were selected according  
169 to their contribution as variable in the component prediction in PLS-DA model, described as Variable  
170 Importance in Projection parameter (VIP), considering only variables with VIP values higher than 1  
171 indicative of significant differences between groups.  
172 Predictability performance was evaluated for each built PLS-DA model. To assess the statistical significance,  
173 t-tests were performed on each metabolite intensities difference between reference and Zn exposed samples,  
174 after normality and homoscedasticity were previously checked. Otherwise, Mann-Whitney tests were  
175 performed.

176  
177  
178

## 179 *Identification and relative level of metabolites*

180 The identification of metabolites was performed by using the human metabolome database  
181 (<http://www.hmdb.ca>) and the METLIN database  
182 ([https://metlin.scripps.edu/landing\\_page.php?pgcontent=mainPage](https://metlin.scripps.edu/landing_page.php?pgcontent=mainPage)) and also for lipids and lipid-derivatives  
183 with the online lipid database: ([http://www.lipidmaps.org/tools/ms/LMSD\\_search\\_mass\\_options.php](http://www.lipidmaps.org/tools/ms/LMSD_search_mass_options.php)). A  
184 research was performed with the mass value of metabolites and a limit with a mass error lower 5 ppm.  
185 Moreover, for succinate and L-phenylalanine, analytical standards were used with the LC/MS method to  
186 verify this identification. Metabolites were finally expressed in relative abundance, which was calculated for  
187 each metabolite by dividing the abundance in each sample by the median abundance across all the samples.

188

189

## 190 **Results**

191

### 192 *Data processing*

193 Mass spectrometry untreated analyses detected 20 946 *m/z* features for negative ionisation mode results in  
194 LC/MS and 44 256 for positive ionisation mode. These large sets of data obtained for metabolomics profiling  
195 were preprocessed applying a Lowess regression model fitting with the pool values as batch correction (Van  
196 Der Kloet et al., 2009).

197 After preprocessing and removal of metabolites with  $CV > 0.4$  in QC samples, the database of metabolites  
198 counted for 1556 and 3581 compounds detected with negative and positive ionisation modes in LC/MS  
199 respectively.

200

### 201 *PCA Analysis*

202 PCA was performed as a first method to confirm differences in metabolite levels between reference animals  
203 and animals exposed to zinc and detect eventual outlier samples. The score plots of PCA analysis are shown  
204 in Figure 1. Each symbol represented an individual sample, and the dot scattering indicated similarities or  
205 differences in metabolic compositions between samples. PCA performed with data sets from both reference  
206 and exposed individuals showed that two groups were well separated according to Zn exposure for the  
207 negative mode but fairly well separated for the positive mode, due to a high dispersion of Zn-exposed  
208 samples along the 2<sup>nd</sup> axis. Thus, the intensities of the compounds, considered as variables, contributed to the  
209 separate structure observed between reference and exposed individuals. The two first axes accounted for  
210 31%-12% and 24%-14% of the total variability among samples for negative and positive data sets  
211 respectively. Reference samples and samples exposed to Zn were grouped and distinguished mainly along  
212 the second axis (*t*<sub>2</sub>) for both ionisation conditions. The model fitted the data well. However, too many  
213 variables were considered to highlight a specific contribution to the total variability within both data sets.

214 Hotelling's  $T^2$  statistic tested the presence of outliers measuring the variation within the PCA model.  
215 Samples with large Hotelling  $T^2$  had an unusual variation inside the model. In this case, they were not  
216 representative of the modeled data and can be considered as outliers if  $p$ -value  $< 0.05$ . The PCA results  
217 showed one outlier sample in the negative mode of data sets (Zn48-2). This outlier sample was removed  
218 from sample matrix data set to perform PLS-DA.

219  
220 *PLS-DA analyses*  
221 PLS-DA analyses were then performed, to identify metabolites whose abundance was related to exposure to  
222 Zn (Figure 1). The first PLS-DA models were built to force the separation between the two populations in  
223 the two datasets. (negative and positive modes). The performances of the model were proven, as the results  
224 of both analyses in negative and positive modes showed a relative data consistency with  $R^2$  (cumulative) =  
225 0.99 and 0.99, respectively. Moreover, the prediction performance of the models reached  $Q^2$  (cumulative) =  
226 0.88 and 0.57 for negative and positive modes respectively, which corresponds to good prediction capability.  
227 However, the permutation test was not significant ( $p$ -value  $> 0.05$ ) for these first models due to the very  
228 large number of variables. In order to improve the prediction performance of the model and to select the  
229 variables with the largest contribution, successive PLS-DA models were built by selecting each time only the  
230 variables with VIPs  $> 1$ . This process was stopped when model predictive performance stopped to increase.  
231 In the negative mode data set, a total of three successive models selecting 465, 155 and 59 metabolites with  
232 VIPs  $> 1$  were performed reaching  $Q^2 = 0.931$ . In the positive mode data set, three successive models  
233 selecting 360, 137 and 40 metabolites with VIPs  $> 1$  were performed reaching  $Q^2 = 0.959$ .  
234 All these selected metabolites showed a significant difference between the reference samples and the  
235 samples exposed to Zn (t-test or Mann-Whitney test,  $p$ -value  $< 0.05$ ).

236  
237 *Metabolite modulation*  
238 Mass-matching analysis using the different online metabolome databases mentioned above or comparison  
239 with standards allowed putative annotation of eleven metabolites showing a significant difference between  
240 reference and Zn exposed samples (Table 1).  
241 Interestingly, all of them were down-modulated when going to references to Zn exposed samples. The  
242 relative abundance of all these metabolites decreased under zinc exposure by more than 30% (Figure 2) : L-  
243 phenylalanine (-39.02%,  $p = 0.05$ ), L-kynurenine (-70.31%,  $p = 0.0038$ ), picolinic acid (-61.93%,  $p = 0.013$ ),  
244 neuroprostane 1 (-58.61%,  $p = 0.027$ ), neuroprostane 2 (identified as 14-hydroperoxy-H4-neuroprostane or  
245 11-hydroperoxy-H4-neuroprostane or 10-hydroperoxy-H4-neuroprostane) (-40.22%,  $p = 0.05$ ),  
246 neuroprostane 3 (256 candidates corresponding to neuroprostanes on 266 entries on lipid maps databank for  
247 this  $m/z$ ) (-52.28%,  $p = 0.05$ ), succinate (-42%,  $p = 0.05$ ), S-(PGA2)-glutathione or S-(PGJ2)-glutathione  
248 (-64.07%,  $p = 0.012$ ), xanthine (-46.65%,  $p = 0.018$ ), hexanoylcarnitine (-36.81%,  $p = 0.044$ ),  
249 dodecenoylcarnitine (-49.12%,  $p = 0.0005$ ).

250



251  
252 **Discussion**  
253 Scallops exposed for 48 h to a nominal zinc concentration of 150  $\mu\text{g}\cdot\text{L}^{-1}$  in laboratory conditions undergo  
254 alterations of their metabolism. These alterations correspond to metabolism of two amino acids (e.g. L-  
255 phenylalanine and L-tryptophan), bioactive lipid compounds (glutathione conjugated prostaglandin and  
256 neuroprostanes), purine metabolism (e.g. xanthine), tricarboxylic acid (TCA) cycle intermediates (succinate)  
257 and metabolism of fatty acids (hexanoylcarnitine and dodecenoylcarnitine). These variations could reflect  
258 potential effects on several of the biological processes discussed below, such as energy metabolism,  
259 including means to face increased energy demand and potential mitochondrial dysfunction, osmoregulation,  
260 oxidative stress defense and purine and tryptophan metabolism as discussed below.  
261 It should be mentioned that the decrease in phenylalanine could also result from disturbed food intake under  
262 stress induction.  
263  
264 *Energy and fatty acid metabolism*  
265 In the present study the decrease of four metabolites (L-phenylalanine, hexanoylcarnitine, trans-2-  
266 dodecenoylcarnitine and succinate) for Zn exposed scallops, may be related with energy metabolism.  
267 The decrease of phenylalanine may reflect its consumption as substrate for energy metabolism, in place of  
268 carbohydrates or lipids, which are used in normal circumstances. Indeed, phenylalanine is an amino acid  
269 being both glucogenic and ketogenic and it can be consumed under energy deficient conditions in aquatic  
270 invertebrates (Sokolova et al., 2012). In case of Zn exposure, this energy deficiency may arise from an  
271 elevated basal metabolic demand due to the need to develop protective mechanisms for the cells, such as  
272 overproduction of metallothioneins, glutathione, molecular chaperones, antioxidants pathways (Cherkasov,  
273 2006; Ivanina et al., 2008; Sokolova and Lannig, 2008). Moreover, toxic metals such as cadmium, copper,  
274 zinc and mercury have been shown to reduce mitochondrial efficiency and coupling and elevated proton leak  
275 in marine organisms (Sokolova et al., 2012). In the same vein, after 9 days of exposure with nominal Zn  
276 concentration of 30  $\mu\text{g}\cdot\text{L}^{-1}$ , oysters gills were analysed by proteomic analysis and it was concluded that Zn  
277 affected the TCA cycle by influencing the expressions of Fe-containing proteins and disrupted the electron  
278 transport chain by inhibiting complex I–IV related protein expressions (Meng et al., 2017). It should be  
279 mentioned that other stress factors such as hypoxia, the presence of other pollutants or high temperature  
280 could concomitantly modify the effect of zinc on the metabolism of bivalves. Recently Belivermis et al.  
281 (2020) showed that hypoxia diminished the Ag and Zn uptake in mussels and induced significantly greater  
282 abundance of several amino acids, amino sulfonic acids, dicarboxylic acids, carbohydrates and other  
283 metabolites compared to Zn exposed mussels in normoxia. Sokolov et al. (2019) observed a decrease of  
284 protein synthesis during hypoxia in intertidal oysters *Crassostrea gigas* and interpreted this as an energy-  
285 saving mechanism.  
286 Two different acylcarnitine, hexanoylcarnitine and trans-2-dodecenoylcarnitine, were found to be down-  
287 regulated in presence of zinc. The first derivative of carnitine (hexanoylcarnitine) is a medium-chain

288 acylcarnitine, whereas the second one (trans-2-dodecenoylcarnitine) is a long-chain acylcarnitine. Long  
289 chain fatty acids have to be combined with carnitine to enter the mitochondria, where they undergo beta-  
290 oxidation for energy production. In contrast, the medium-chain fatty acids can enter the mitochondrial  
291 membrane directly for beta-oxidation without the need of carnitine-mediated transport. Therefore, in our  
292 case, the defect of trans-2-dodecenoylcarnitine mainly affects the oxidation of the corresponding long-chain  
293 fatty acids. However, the metabolism of acylcarnitines is not only related to the transport of fatty acids, but  
294 also plays a key role in maintaining the homeostasis of the mitochondrial acyl-CoA/CoA ratio (Connor and  
295 Gracey, 2012; Gracey and Connor, 2016) and in other physiological processes such as peroxidation of fatty  
296 acids. Therefore, the observed change in acylcarnitine profile in presence of zinc may be related more  
297 generally with potential mitochondrial dysfunction and abnormal fatty acid metabolism.

298 Lastly, succinate was found to decrease upon Zn exposure. It is a metabolite intermediate of the TCA cycle,  
299 which is oxidized into fumarate by the iron-sulfur enzyme succinate dehydrogenase (SDH). Zn affects the  
300 TCA cycle by influencing the expressions of Fe-containing proteins (Pagani et al., 2007) and it is therefore  
301 so not surprising to observe that succinate is impacted by Zn in our study. What is more surprising is that the  
302 succinate appears in the present study to be down-regulated after Zn exposure. Indeed, in several previous  
303 studies, an accumulation of succinate was observed after Zn exposure : in the gills of Pacific oyster  
304 (*Crassostrea gigas*) exposed to excess Zn solution (30  $\mu\text{g.L}^{-1}$ ) for 9 days (Meng et al., 2017), in the digestive  
305 gland of *Ruditapes philippinarum* exposed to  $\text{ZnCl}_2$  (nominal concentrations: 20, 50, 100 and 150  $\mu\text{g.L}^{-1}$ ) for  
306 48 h (Aru et al., 2016) and in adductor muscles of the pedigree White clam of *Ruditapes philippinarum* after  
307 exposure with  $\text{Zn}^{2+}$  (50  $\mu\text{g.L}^{-1}$ ) for 48 h (Wu et al., 2011). This accumulation of succinate was interpreted as  
308 molecular sign of the shift in cellular metabolism to anaerobiosis. It was explained in details by proteomic  
309 analysis, by a decrease in SDH expression and a simultaneously increase in enzyme succinyl-CoA synthetase  
310 (SCS) expression, which allows succinate biosynthesis in the TCA cycle, under Zn exposure of oysters  
311 (Meng et al., 2017). Nevertheless, in the same study, fumarase (FUM), another Fe-S enzyme that converts  
312 fumarate to L-malate in the TCA cycle, showed significantly increased levels of expression at the same time.  
313 This was interpreted as a compensation mechanism for ensuring that the TCA cycle remains active when  
314 exposed to metals (Meng et al., 2017). This indicates that Fe-S enzymes of the TCA cycles can be either up-  
315 or down-regulated upon Zn exposure and that defense strategy against Zn toxicity exists in bivalves, as it is  
316 the case with bacteria exposed to metals such as Al that interfere with Fe metabolism (Chenier et al., 2008).

317 In another study, two pedigrees (White and Zebra) of clam *Ruditapes philippinarum* were exposed with  
318  $\text{Zn}^{2+}$ (50  $\mu\text{g.L}^{-1}$ ) during 48 h and the metabolomics results showed differences in digestive gland between  
319 White and Zebra clam samples in succinate levels: in Zebra clam, succinate was increased, whereas it was  
320 decreased in White clam after Zn exposure (Ji et al., 2015). In conclusion, it seems clear that Zn affects the  
321 TCA cycle metabolites, through its effect on Fe-S enzymes involved in the cycle. Concerning the level of  
322 succinate, it may be increased or decreased upon Zn exposure, depending on the species, with respect to  
323 over- or under-expression of the different Fe-S enzymes of the TCA cycle.

324 However, succinate has multiple roles in cell metabolism and its decrease may be linked among others with  
325 formation and elimination of reactive oxygen species, as discussed below.

326

### 327 *Osmoregulation*

328 Down-modulation of L-phenylalanine on the one hand and of prostaglandine-glutathione and neuroprostanes  
329 on the other hand, in Zn exposed scallops may be related to osmoregulation phenomena.

330 Indeed, L-phenylalanine is a catecholamine precursor and its lower level may lead to a decrease in  
331 dopamine. Dopamine and serotonin are neurotransmitters involved in the modulation of Na<sup>+</sup> and K<sup>+</sup> transport  
332 in gills of crustaceans (Mo et al., 1998) and in lateral cilia in gills of bivalves (Carroll and Catapane, 2007).  
333 The down-modulation of dopamine may thus have a repercussion on osmoregulation of cells submitted to Zn  
334 exposure. A similar relationship between L-phenylalanine decrease and osmoregulation was previously  
335 suggested (Aru et al., 2016). These authors observed a down-modulation of phenylalanine in presence of  
336 ZnCl<sub>2</sub> (20, 50, 100 and 150 µg.L<sup>-1</sup>) under laboratory conditions after 48 h exposure for the clam *Ruditapes*  
337 *decussatus*, associated with a significant increment in organic osmolyte production (hypotaurine and  
338 homarine) and a decrease of the content of free amino acid.

339 Prostaglandins (PGs) are an important group of bioactive lipid compounds in living organisms; they are  
340 involved in mammals in a great variety of physiopathological processes like for instance inflammation,  
341 signaling or reproduction. These molecules play similar roles in marine invertebrates, being involved in the  
342 control of gametogenesis, ion transport, and defense. These molecules also represent very important lipid  
343 mediators in marine invertebrates (Di Costanzo et al., 2019). PGs biosynthesis starts with arachidonic acid, a  
344 polyunsaturated fatty acid (PUFA), that is oxidised by enzymes such as cyclooxygenase or lipoxygenase to  
345 give precursors, which are then further transformed by a large number of possible enzymes, giving rise to the  
346 formation of different families of PGs, like PG J<sub>2</sub> and PGA<sub>2</sub>. These last PGs may undergo addition reactions  
347 with glutathione (GSH) to give new reactive compounds in humans (Murphy and Zarini, 2002). In the  
348 present study, among the metabolites showing a down regulation after 48 h Zn exposure, a compound  
349 putatively identified as S-(PGA<sub>2</sub>)-glutathione or S-(PGJ<sub>2</sub>)-glutathione was obtained. This would indicate  
350 that these types of conjugates are also present in bivalves and are impacted by exposure to Zn.

351 Isoprostanes (IsoPs) and the IsoP-like molecules are PG-like compounds formed *in vivo* via the  
352 nonenzymatic free radical-initiated peroxidation of a number of different PUFAs. Among them,  
353 neuroprostanes (MPs) are generated from the PUFA docosahexaenoic acid (DHA) (Milne et al., 2011). PGs,  
354 IsoPs and IsoP-like molecules have been identified recently in molluscs (Bonfille et al., 2018; Chakraborty  
355 et al., 2014), which is not surprising given that PUFAs are essential molecules for the survival of bivalves  
356 (Da Costa et al., 2015) and that they are highly susceptible to oxidation because of the large number of their  
357 double bonds.

358 The role of PGs, IsoPs and Iso-P like molecules in invertebrates has not yet been fully elucidated. Some  
359 studies show that they have a role in osmoregulation : PGE<sub>2</sub> was shown to be involved in Na transport  
360 regulation in gills of the freshwater mussel *Ligumia subrostrata* and also in clams (Saintsing and Dietz, 1983)

361 and it was shown that hyposmotic stress significantly increased prostaglandin synthesis in the marine bivalve  
362 *Modiolus demissus* (Freas and Grollman, 1980). In the present case, a down-modulation of three compounds  
363 identified as neuroprostanes was obtained after Zn exposure and this may be linked also with  
364 osmoregulation. In fish, prostaglandins were shown to be involved in Cl<sup>-</sup> secretion (Avella et al., 1999) and  
365 effluent exposure resulted also in widespread reduction (between 50% and 90%) in PG profiles obtained  
366 through metabolomics in fish tissues and plasma (David et al., 2017).

367

#### 368 *Oxidative stress defense*

369 Besides their possible role in the above mentioned osmoregulation, IsoPs and Iso-P like molecules have  
370 become biomarkers of choice in human for assessing endogeneous oxidative stress linked with many  
371 pathological disorders, because they are chemically stable (Milne et al., 2008). Oxidative stress is  
372 characterised by an imbalance between cellular antioxidant defenses and overproduction of free radicals,  
373 particularly reactive species of oxygen (ROS). Lipids are readily attacked by free radicals, resulting in the  
374 formation of a number of peroxidation products. In bivalves, like in other animals, there is a close  
375 relationship between environmental stress and the rate of cellular ROS generation and consequently lipid  
376 peroxidation reactions (Regoli and Giuliani, 2014). In our case, the modification of the Iso-P like molecules  
377 profile could therefore be linked to an increased oxidative stress in the presence of Zn.

378 Another down-modulated metabolite under Zn exposure that may be linked with oxidative stress defense is  
379 succinate. The roles of succinate in mitochondrial ROS formation and elimination are numerous and  
380 complex (Tretter et al., 2016). It was shown that succinate exerted an inhibitory effect on lipid peroxidation  
381 in mitochondria. This protective role of succinate against oxidation was attributed to the maintenance of a  
382 pool of reduced coenzyme Q. Succinate was oxidised by the membrane-bound succinate dehydrogenase and  
383 the enzyme activity was only moderately sensitive to oxidants, therefore it was more efficient in maintaining  
384 reduced coenzyme Q, thus maintaining membrane integrity.

385 Other metals and in particular copper are able to induce oxidative stress in bivalves. Cu<sup>2+</sup>-exposed  
386 haemocytes showed a remarkable increase in ROS production, which induced oxidative stress in mussel  
387 (*Perna canaliculus*) (Nguyen et al., 2018). This was accompanied by a decrease in GSH. This compound is  
388 an important antioxidant, able to react with electrophilic oxidants (e.g., H<sub>2</sub>O<sub>2</sub>) resulting in conversion of two  
389 GSH molecules into its oxidized form (GSSG). Two other molecules decrease simultaneously upon Cu<sup>2+</sup>  
390 exposure: cysteine, which is involved in the GSH metabolic pathway and methionine, which takes place in  
391 the transsulfuration pathway, a source of cysteine for GSH. These concomitant phenomena were identified as  
392 important signatures of oxidative stress (Nguyen et al., 2018).

393

#### 394 *Purine metabolism*

395 A lower level of xanthine in presence of Zn suggests a disordered nucleotide metabolism. Indeed, in the  
396 catabolism of purine nucleotides, adenosine monophosphate (AMP) and guanosine monophosphate (GMP)  
397 both lead to xanthine (Van Waarde, 1988). AMP is degraded to inosine and then by phosphorolysis to

398 hypoxanthine. In presence of xanthine oxidase (XOD), xanthine is formed from oxidation of hypoxanthine.  
399 GMP is degraded to guanosine and then by phosphorolysis to guanine, which is transformed to xanthine by  
400 guanine deaminase. This makes the metabolic interrelationships between nucleotides and purine base  
401 nucleosides, and finally xanthine, very strong (Harkness, 1988). Therefore, we can consider that xanthine is  
402 at the center of the interplay between ATP and GTP metabolism. Since the nucleotides ATP and GTP are the  
403 energy carriers molecules in cells, it can be hypothesised that zinc would induce an increased demand for  
404 energy by the cells.

405 Previously, a decrease of inosine (between -30 and -80%) and hypoxanthine (between -40 and -50%) was  
406 observed in whole body of zebrafish, after exposure to ZnCl<sub>2</sub> at different concentrations (10, 100, 500 and  
407 1000 µg.L<sup>-1</sup> for 72 h). It was interpreted as an impairment of the purine metabolism caused by exposure to  
408 Zn. As it was combined with an ATP level increased, it was hypothesised that Zn would induce an increased  
409 energy demand to fulfil essential maintenance costs and ensure organism survival (e.g. cellular protective  
410 mechanisms, detoxification) (Kim et al., 2016; Sokolova et al., 2012).

#### 411 412 *Tryptophan metabolism*

413 In humans, L-tryptophan is metabolised by two main pathways : the serotonin pathway (around 1% of L-  
414 tryptophan metabolism) and the kynurenine pathway (around 95% of L-tryptophan metabolism). In the  
415 kynurenine pathway, L-tryptophan gives one of three main end products: kynurenic acid, picolinic acid and  
416 NAD. This pathway begins with the oxidative cleavage of L-tryptophan by either one of the two enzymes  
417 indoleamine 2,3-dioxygenase (IDO) or tryptophan 2,3-dioxygenase also called tryptophan pyrrolase (TDO) to  
418 produce L-formylkynurenine, which is then converted to L-kynurenine by a formamidase. L-kynurenine is a  
419 branch point and can be converted to the following: 1) kynurenic acid by kynurenine aminotransferases; 2)  
420 3-hydroxykynurenine by kynurenine 3-monooxygenase; or 3) anthranilic acid. 3-hydroxykynurenine further  
421 undergoes enzymatic or chemical transformations to give either picolinic acid or NAD (Grant et al., 2009).  
422 The kynurenine metabolism was shown to be highly conserved throughout evolution and the enzyme IDO  
423 was discovered in mammals, lower vertebrates, several invertebrates, fungi and a number of bacterial species  
424 (Cervenka et al., 2017).

425 In the present study, a down-regulation of both picolinic acid and kynurenine was observed after Zn  
426 exposure, showing an impact of this metal on tryptophan metabolism. This trend was also observed in  
427 another study with the marine bivalve *Mytilus galloprovincialis*, when exposed to a wastewater treatment  
428 plants effluent extract: both L-formylkynurenine and L-kynurenine were found to be down-regulated  
429 (respectively -55%,  $p \leq 0.05$  and -63%,  $p \leq 0.05$ ) compared to non-exposed animals thanks to a non-targeted  
430 metabolomics study (Dumas et al., 2020).

431 In another study using proteomic analysis with the pacific oyster *Crassostrea gigas* the enzyme kynurenine  
432 formamidase was found to be down-regulated under aerial exposure (Zhang et al., 2015), which again  
433 corresponds to an impairment of the tryptophan metabolism. This was accompanied by the suppression of

434 many physiological activities and this was interpreted as a means of redistributing available resources to fuel  
435 stress responses (Zhang et al., 2015).

436

### 437 **Conclusion**

438 In the present study, we chose the variegated scallop *Mimachlamys varia*, for assessing zinc contamination  
439 effects on their metabolism, at a concentration such as the one the metal can reach in La Rochelle marina. An  
440 untargeted UHPLC/QToF tandem mass spectrometry metabolomics approach was chosen, as it offers a high  
441 level of sensitivity to highlight impacts due to short-time metal exposure. Metabolite profiling of gills tissues  
442 could clearly separate scallops with no metal inputs and those exposed to 48 h zinc exposure, under  
443 laboratory conditions. Among the high quantity of modulated metabolites, only a few of them were  
444 identified, because of the current lack of knowledge on scallop metabolism. They include amino acids or  
445 their metabolites, bioactive lipid compounds, including four metabolites never before identified in bivalves,  
446 metabolites of purine or the TCA cycle and carnitine conjugates of fatty acids. These molecules reflect  
447 potential zinc effects on several of the biological processes, such as energy metabolism, osmoregulation,  
448 defense against oxidative stress, metabolism of purine and tryptophan.

449 This study demonstrates once again that metabolomics approach, when used in untargeted mode is able to  
450 reveal novel and unanticipated physiological perturbations, without *a priori* knowledge of the metabolome.  
451 This is valuable in the present case where a poorly studied animal model is used. The limitations of the  
452 technique come from the fact that there are a large number of unknown metabolites that remain unannotated  
453 in the databases, so that some metabolite features cannot be attributed to a molecular structure. The  
454 development of new methods dedicated to the identification of metabolites on the one hand and to the search  
455 for the connectivity of metabolic pathways on the other hand, combined with the enrichment of databases,  
456 will make it possible in the future to carry out more and more advanced impact analyses.

457 Moreover, further study is needed to assess the effect of other trace elements present in the marine  
458 environment and better understand the combined effects of pollutants. La Rochelle marina sets up multiple  
459 actions to ensure a sustainable development of coastal activities while preserving the aquatic environment.  
460 These actions, framed by the "Ports Propres" AFAQ certification (AFNOR : Association française de  
461 normalisation), are based on criteria approved at the European level by the CWA 16987 agreement of the  
462 "Clean Harbour Guidelines". Among them, some aim to develop approaches to highlight the physiological  
463 modifications of marine organisms impacted by environmental variation. Our results show that  
464 metabolomics is a powerful method that can brings out small environmental variations, such as zinc  
465 concentration, through metabolic changes in scallops.

466

### 467 **Acknowledgements**

468 We gratefully thank E. Dubillot (from laboratory "Littoral Environnement et Sociétés" (LIENSs), UMR  
469 7266, CNRS-Université de La Rochelle, 2 rue Olympe de Gouges, F-17042 La Rochelle Cedex 01, France)

470 for technical assistance. We also thank the Marina of La Rochelle for their assistance in particularly for the  
471 data transmission and the “Musée Mer Marine Bordeaux” for the involvement in the V. HAMANI PhD.

472

### 473 **Funding sources**

474 Funding for this work came from the following separate sources: (i) Contrat de Plan Etat-Région FEDER  
475 and the CNRS ECONAT Axe 1 - Ressources Marines Littorales: qualité et éco-valorisation and Axe 2 -  
476 Gestion Intégrée des Zones Littorales et Portuaires (ii) French Ministry of Higher Education, Research and  
477 Innovation for doctoral grant of V. Hamani (Ministère de l'Enseignement supérieur, de la Recherche et de  
478 l'Innovation, MESRI).

479

### 480 REFERENCES

- 481 Aru, V., Sarais, G., Savorani, F., Engelsen, S.B., Cesare Marincola, F., 2016. Metabolic responses of clams,  
482 *Ruditapes decussatus* and *Ruditapes philippinarum*, to short-term exposure to lead and zinc. Mar.  
483 Pollut. Bull. 107, 292–299. <https://doi.org/10.1016/j.marpolbul.2016.03.054>
- 484 Avella, M., Pärt, P., Ehrenfeld, J., 1999. Regulation of Cl<sup>-</sup> secretion in seawater fish (*Dicentrarchus labrax*)  
485 gill respiratory cells in primary culture. J. Physiol. 516, 353–363. <https://doi.org/10.1111/j.1469-7793.1999.0353v.x>
- 487 Bighiu, M.A., Gorokhova, E., Carney Almroth, B., Eriksson Wiklund, A.-K., 2017. Metal contamination in  
488 harbours impacts life-history traits and metallothionein levels in snails. PLoS ONE 12, e0180157.  
489 <https://doi.org/10.1371/journal.pone.0180157>
- 490 Belivermis, M., Swarzenski, P.W., Oberhänsli, F., Melvin S.D., Metian, M., 2020. Effects of variable deoxygenation  
491 on trace element bioaccumulation and resulting metabolome profiles in the blue mussel (*Mytilus edulis*).  
492 Chemosphere 250, 126314.
- 493 Bonnefille, B., Gomez, E., Alali, M., Rosain, D., Fenet, H., Courant, F., 2018. Metabolomics assessment of  
494 the effects of diclofenac exposure on *Mytilus galloprovincialis*: Potential effects on osmoregulation  
495 and reproduction. Sci. Total Environ. 613–614, 611–618.  
496 <https://doi.org/10.1016/j.scitotenv.2017.09.146>
- 497 Booth, S.C., Workentine, M.L., Weljie, A.M., Turner, R.J., 2011. Metabolomics and its application to studying metal  
498 toxicity. Metallomics. 3, 1142–1152. doi:10.1039/c1mt00070e.
- 499 Breitwieser, M., Becquet, V., Thomas-Guyon, H., Pillet, V., Sauriau, P.-G., Graber, M., Viricel, A., 2018a.  
500 Population structure and genetic diversity in the variegated scallop, *Mimachlamys varia* (Linnaeus,  
501 1758), a novel bioindicator of chemical pollution on the French coastline. J. Molluscan Stud. 84,  
502 417–425. <https://doi.org/10.1093/mollus/eyy035>
- 503 Breitwieser, M., Vigneau, E., Viricel, A., Becquet, V., Lacroix, C., Erb, M., Huet, V., Churlaud, C., Le  
504 Floch, S., Guillot, B., Graber, M., Thomas, H., 2018b. What is the relationship between the  
505 bioaccumulation of chemical contaminants in the variegated scallop *Mimachlamys varia* and its  
506 health status? A study carried out on the French Atlantic coast using the Path ComDim model. Sci.  
507 Total Environ. 640–641, 662–670. <https://doi.org/10.1016/j.scitotenv.2018.05.317>
- 508 California Stormwater Quality Association [CASQA], (2015), Zinc Sources in California Urban Runoff,  
509 Retrieved from [https://www.casqa.org/sites/default/files/library/technical-](https://www.casqa.org/sites/default/files/library/technical-reports/zinc_sources_in_california_urban_runoff.pdf)  
510 [reports/zinc\\_sources\\_in\\_california\\_urban\\_runoff.pdf](https://www.casqa.org/sites/default/files/library/technical-reports/zinc_sources_in_california_urban_runoff.pdf)
- 511 Carroll, M.A., Catapane, E.J., 2007. The nervous system control of lateral ciliary activity of the gill of the  
512 bivalve mollusc, *Crassostrea virginica*. Comp. Biochem. Physiol. A. Mol. Integr. Physiol. 148, 445–  
513 450. <https://doi.org/10.1016/j.cbpa.2007.06.003>
- 514 Cervenka, I., Agudelo, L.Z., Ruas, J.L., 2017. Kynurenines: Tryptophan's metabolites in exercise,  
515 inflammation, and mental health. Science 357, eaaf9794. <https://doi.org/10.1126/science.aaf9794>

516 Chakraborty, K., Chakkalakal, S.J., Joseph, D., 2014. Response of pro-inflammatory prostaglandin contents  
517 in anti-inflammatory supplements from green mussel *Perna viridis* L. in a time-dependent  
518 accelerated shelf-life study. *J. Funct. Foods* 7, 527–540. <https://doi.org/10.1016/j.jff.2014.01.003>

519 Chenier, D., Bériault, R., Mailloux, R., Baquie, M., Abramia, G., Lemire, J., Appanna, V., 2008.  
520 Involvement of Fumarase C and NADH Oxidase in Metabolic Adaptation of *Pseudomonas*  
521 *fluorescens* Cells Evoked by Aluminum and Gallium Toxicity. *Appl. Environ. Microbiol.* 74, 3977–  
522 3984. <https://doi.org/10.1128/AEM.02702-07>

523 Cherkasov, A.S., 2006. Effects of acclimation temperature and cadmium exposure on cellular energy budgets  
524 in the marine mollusk *Crassostrea virginica*: linking cellular and mitochondrial responses. *J. Exp.*  
525 *Biol.* 209, 1274–1284. <https://doi.org/10.1242/jeb.02093>

526 Connor, K.M., Gracey, A.Y., 2012. High-resolution analysis of metabolic cycles in intertidal mussel *Mytilus*  
527 *californianus*. *Am. J. Physiol.-Regul. Integr. Comp. Physiol.* 302, 103–111.

528 CREOCEAN (2018) Suivi des rejets des activités de carénage – Port de plaisance des Minimes (report  
529 N°170833)-18p

530 Da Costa, F., Robert, R., Quéré, C., Wikfors, G.H., Soudant, P., 2015. Essential Fatty Acid Assimilation and  
531 Synthesis in Larvae of the Bivalve *Crassostrea gigas*. *Lipids* 50, 503–511.  
532 <https://doi.org/10.1007/s11745-015-4006-z>

533 David, A., Lange, A., Abdul-Sada, A., Tyler, C.R., Hill, E.M., 2017. Disruption of the Prostaglandin  
534 Metabolome and Characterization of the Pharmaceutical Exposome in Fish Exposed to Wastewater  
535 Treatment Works Effluent As Revealed by Nanoflow-Nanospray Mass Spectrometry-Based  
536 Metabolomics. *Environ. Sci. Technol.* 51, 616–624. <https://doi.org/10.1021/acs.est.6b04365>

537 Di Costanzo, F., Di Dato, V., Ianora, A., Romano, G., 2019. Prostaglandins in Marine Organisms: A Review. *Marine*  
538 *Drugs* 17, 428-451. <https://doi.org/10.3390/md17070428>

539 Dumas, T., Bonnefille, B., Gomez, E., Bocard, J., Castro, N.A., Fenet, H., Courant, F., 2020. Metabolomics  
540 approach reveals disruption of metabolic pathways in the marine bivalve *Mytilus galloprovincialis*  
541 exposed to a WWTP effluent extract. *Sci. Total Environ.* 712, 136551.  
542 <https://doi.org/10.1016/j.scitotenv.2020.136551>

543 Eklund, B., Eklund, D., 2014. Pleasure Boatyard Soils are Often Highly Contaminated. *Environ. Manage.* 53,  
544 930–946. <https://doi.org/10.1007/s00267-014-0249-3>

545 Freas, W., Grollman, S., 1980. Ioninc and osmotic influences on prostaglandin release from the gill tissue of  
546 a marine bivalve, *Modiolus demissus*. *J. Exp. Biol.* 84, 169–185.

547 Galkus, A., Joksas, K., Stakeniene, R., Lagunaviciene, L., 2012. Heavy Metal Contamination of Harbor  
548 Bottom Sediments. *Pol. J. Environ. Stud.* 21, 1583–1594.

549 Gracey, A.Y., Connor, K., 2016. Transcriptional and metabolomic characterization of spontaneous metabolic  
550 cycles in *Mytilus californianus* under subtidal conditions. *Mar. Genomics* 30, 35–41.  
551 <https://doi.org/10.1016/j.margen.2016.07.004>

552 Grant, R.S., Coggan, S.E., Smythe, G.A., 2009. The Physiological Action of Picolinic Acid in the Human  
553 Brain. *Int. J. Tryptophan Res.* 2, IJTR.S2469. <https://doi.org/10.4137/IJTR.S2469>

554 Harkness, R.A., 1988. Hypoxanthine, xanthine and uridine in body fluids, indicators of ATP depletion. *J.*  
555 *Chromatogr. B. Biomed. Sci. App.* 429, 255–278. [https://doi.org/10.1016/S0378-4347\(00\)83873-6](https://doi.org/10.1016/S0378-4347(00)83873-6)

556 Huguet, J.-R.; Brenon, I.; Coulombier, T. 2019. Characterisation of the water renewal in a macro-tidal marina using  
557 several transport timescales. *Water*, 11, 2050-2073.

558 Ivanina, A.V., Cherkasov, A.S., Sokolova, I.M., 2008. Effects of cadmium on cellular protein and glutathione  
559 synthesis and expression of stress proteins in eastern oysters, *Crassostrea virginica* Gmelin. *J. Exp. Biol.* 211,  
560 577–586. <https://doi.org/10.1242/jeb.011262>

561 Ji, C., Cao, L., Li, F., 2015. Toxicological evaluation of two pedigrees of clam *Ruditapes philippinarum* as  
562 bioindicators of heavy metal contaminants using metabolomics. *Environ. Toxicol. Pharmacol.* 39,  
563 545–554. <https://doi.org/10.1016/j.etap.2015.01.004>

564 Johnston, E.L., Marzinelli, E.M., Wood, C.A., Speranza, D., Bishop, J.D.D., 2011. Bearing the burden of  
565 boat harbours: Heavy contaminant and fouling loads in a native habitat-forming alga. *Mar. Pollut.*  
566 *Bull.* 62, 2137–2144. <https://doi.org/10.1016/j.marpolbul.2011.07.009>

567 Kim, S., Yoon, D., Lee, M., Yoon, C., Kim, S., 2016. Metabolic responses in zebrafish (*Danio rerio*)  
568 exposed to zinc and cadmium by nuclear magnetic resonance -based metabolomics. *Chem. Ecol.* 32,  
569 136–148. <https://doi.org/10.1080/02757540.2015.1125891>



570 Lankadurai, B.P., Nagato, E.G., Simpson, M.J., 2013. Environmental metabolomics: an emerging approach to study  
571 organism responses to environmental stressors. *Environ. Rev.* 21, 180–205. [https://doi.org/10.1139/er-2013-](https://doi.org/10.1139/er-2013-0011)  
572 0011.

573 Marigómez, I., Soto, M., Cajaraville, M.P., Angulo, E., Giamberini, L., 2002. Cellular and subcellular distribution of  
574 metals in molluscs. *Microscop. Res. Tech.* 56, 358-392.

575 Meng, J., Wang, W.-X., Li, L., Zhang, G., 2017. Respiration disruption and detoxification at the protein  
576 expression levels in the Pacific oyster (*Crassostrea gigas*) under zinc exposure. *Aquat. Toxicol.* 191,  
577 34–41. <https://doi.org/10.1016/j.aquatox.2017.07.011>

578 Metian, M., Bustamante, P., Hédouin, L., Oberhänsli, F., Warnau, M., 2009a. Delineation of heavy metal  
579 uptake pathways (seawater and food) in the variegated scallop *Chlamys varia*, using radiotracer  
580 techniques. *Mar. Ecol. Prog. Ser.* 375, 161–171. <https://doi.org/10.3354/meps07766>

581 Metian, M., Warnau, M., Oberhänsli, F., Bustamante, P., 2009b. Delineation of Pb contamination pathways  
582 in two Pectinidae: The variegated scallop *Chlamys varia* and the king scallop *Pecten maximus*. *Sci.*  
583 *Total Environ.* 407, 3503–3509. <https://doi.org/10.1016/j.scitotenv.2009.02.010>

584 Milinkovitch, T., Bustamante, P., Huet, V., Reigner, A., Churlaud, C., Thomas-Guyon, H., 2015. *In situ*  
585 evaluation of oxidative stress and immunological parameters as ecotoxicological biomarkers in a  
586 novel sentinel species (*Mimachlamys varia*). *Aquat. Toxicol.* 161, 170–175.  
587 <https://doi.org/10.1016/j.aquatox.2015.02.003>

588 Milne, G.L., Yin, H., Hardy, K.D., Davies, S.S., Roberts, L.J., 2011. Isoprostane Generation and Function.  
589 *Chem. Rev.* 111, 5973–5996. <https://doi.org/10.1021/cr200160h>

590 Milne, G.L., Yin, H., Morrow, J.D., 2008. Human Biochemistry of the Isoprostane Pathway. *J. Biol. Chem.*  
591 283, 15533–15537. <https://doi.org/10.1074/jbc.R700047200>

592 Mo, J.L., Devos, P., Trausch, G., 1998. Dopamine as a modulator of ionic transport and Na<sup>+</sup>/K<sup>+</sup>-ATPase  
593 activity in the gills of the chinese crab *Eriocheir sinensis*. *J. Crustac. Biol.* 18, 442–448.  
594 <https://doi.org/10.1163/193724098X00278>

595 Mondeguer, F., Abadie, E., Herve, F., Bardouil, M., Sechet, V., Raimbault, V., Berteaux, T., Zendong, S.Z.,  
596 Palvadeau, H., Amzil, Z., Hess, P., Fessard, V., Huguet, A., Sosa, S., Tubaro, A., Aráoz, R., Molgó,  
597 J., 2015. Pinnatoxines en lien avec l'espèce *Vulcanodinium rugosum* (II).  
598 <http://archimer.ifremer.fr/doc/00285/39635/>

599 Murphy, R.C., Zarini, S., 2002. Glutathione adducts of oxyeicosanoids. *Prostaglandins Other Lipid Mediat.*  
600 68–69, 471–482. [https://doi.org/10.1016/S0090-6980\(02\)00049-7](https://doi.org/10.1016/S0090-6980(02)00049-7)

601 Nguyen, T.V., Alfaro A.C., Merien F., Lulijwa R., Young T., 2018. Copper-induced immunomodulation in mussel  
602 (*Perna canaliculus*) haemocytes. *Metallomics* 10, 965-978.

603 Ory, P., Bonnet, A., Mondeguer, F., Breitwieser, M., Dubillot, E., Graber, M., 2019. Metabolomics based on  
604 UHPLC-QToF- and APGC-QToF-MS reveals metabolic pathways reprogramming in response to  
605 tidal cycles in the sub-littoral species *Mimachlamys varia* exposed to aerial emergence. *Comp.*  
606 *Biochem. Physiol. Part D Genomics Proteomics* 29, 74–85.  
607 <https://doi.org/10.1016/j.cbd.2018.11.002>

608 Pagani, M.A., Casamayor, A., Serrano, R., Atrian, S., Ariño, J., 2007. Disruption of iron homeostasis in  
609 *Saccharomyces cerevisiae* by high zinc levels: a genome-wide study. *Mol. Microbiol.* 65, 521–537.  
610 <https://doi.org/10.1111/j.1365-2958.2007.05807.x>

611 Pomfret, S.M., Brua, R.B., Izral, N.M., Yates, A.G., 2020. Metabolomics for biomonitoring: an evaluation of the  
612 metabolome as an indicator of aquatic ecosystem health. *Environmental Reviews*, 28, 89-98.

613 Regoli, F., Giuliani, M.E., 2014. Oxidative pathways of chemical toxicity and oxidative stress biomarkers in  
614 marine organisms. *Mar. Environ. Res.* 93, 106–117. <https://doi.org/10.1016/j.marenvres.2013.07.006>

615 Saintsing, D.G., Dietz, T.H., 1983. Modification of sodium transport in freshwater mussels by  
616 prostaglandins, cyclic AMP and 5-hydroxytryptamine: effects of inhibitors of prostaglandin  
617 synthesis. *Comp. Biochem. Physiol. Part C Comp. Pharmacol.* 76, 285–290.  
618 [https://doi.org/10.1016/0742-8413\(83\)90080-4](https://doi.org/10.1016/0742-8413(83)90080-4)

619 Sim, V.X.Y., Dafforn, K.A., Simpson, S.L., Kelaher, B.P., Johnston, E.L., 2015. Sediment Contaminants and  
620 Infauna Associated with Recreational Boating Structures in a Multi-Use Marine Park. *PLoS ONE*  
621 10, e0130537. <https://doi.org/10.1371/journal.pone.0130537>

622 Sokolov, E.P., Markert, S., Hinzkeb, T., Hirschfeld, C., Becher, D., Ponsuksili, S., Inna M. Sokolova I.M., 2019.  
623 Effects of hypoxia-reoxygenation stress on mitochondrial proteome and bioenergetics of the hypoxia-tolerant  
624 marine bivalve *Crassostrea gigas*. *J. Proteomics* 194, 99–111.

625 Sokolova, I.M., Lannig, G., 2008. Interactive effects of metal pollution and temperature on metabolism in  
626 aquatic ectotherms: implications of global climate change. *Clim. Res.* 37, 181–201.  
627 <https://doi.org/10.3354/cr00764>

628 Sokolova, I.M., Frederich, M., Bagwe, R., Lannig, G., Sukhotin, A.A., 2012. Energy homeostasis as an  
629 integrative tool for assessing limits of environmental stress tolerance in aquatic invertebrates. *Mar.*  
630 *Environ. Res.* 79, 1–15. <https://doi.org/10.1016/j.marenvres.2012.04.003>

631 Stankovic, S., Kalaba, P., Stankovic, A.R., 2014. Biota as toxic metal indicators. *Environ. Chem. Lett.* 12,  
632 63–84. <https://doi.org/10.1007/s10311-013-0430-6>

633 Tretter, L., Patocs, A., Chinopoulos, C., 2016. Succinate, an intermediate in metabolism, signal transduction, ROS,  
634 hypoxia, and tumorigenesis. *Biochim. Biophys. Acta* 1857, 1086–1101.

635 Van Der Kloet, F.M., Bobeldijk, I., Verheij, E.R., Jellema, R.H., 2009. Analytical error reduction using  
636 single point calibration for accurate and precise metabolomic phenotyping. *J. Proteome Res.* 8,  
637 5132–5141.

638 Van Waarde, A., 1988. Operation of the purine nucleotide cycle in animal tissues. *Biol. Rev.* 63, 259-298.

639 Viant, M.R., Sommer, U., 2012. Mass spectrometry based environmental metabolomics: a primer and review.  
640 *Metabolomics* 9, 1-15.

641 Wang, W.-Meng, J., Weng, N., 2018. Trace metals in oysters: molecular and cellular mechanisms and  
642 ecotoxicological impacts. *Environ. Sci. Process. Impacts* 20, 892–912. <https://doi.org/10.1039/C8EM00069G>

643 Wu, H., Liu, X., Zhao, J., Yu, J., 2011. NMR-Based Metabolomic Investigations on the Differential  
644 Responses in Adductor Muscles from Two Pedigrees of Manila Clam *Ruditapes philippinarum* to  
645 Cadmium and Zinc. *Mar. Drugs* 9, 1566–1579. <https://doi.org/10.3390/md9091566>

646 Wu, H., Xu, L., Yu, D., and Ji, C. 2017. Differential metabolic responses in three life stages of mussels *Mytilus*  
647 *galloprovincialis* exposed to cadmium. *Ecotoxicology* 26, 74-80. doi:10.1007/s10646-016-1741-8.

648 Zhang, Yang, Sun, J., Mu, H., Li, J., Zhang, Yuehuan, Xu, F., Xiang, Z., Qian, P.-Y., Qiu, J.-W., Yu, Z.,  
649 2015. Proteomic Basis of Stress Responses in the Gills of the Pacific Oyster *Crassostrea gigas*. *J.*  
650 *Proteome Res.* 14, 304–317. <https://doi.org/10.1021/pr500940s>

651

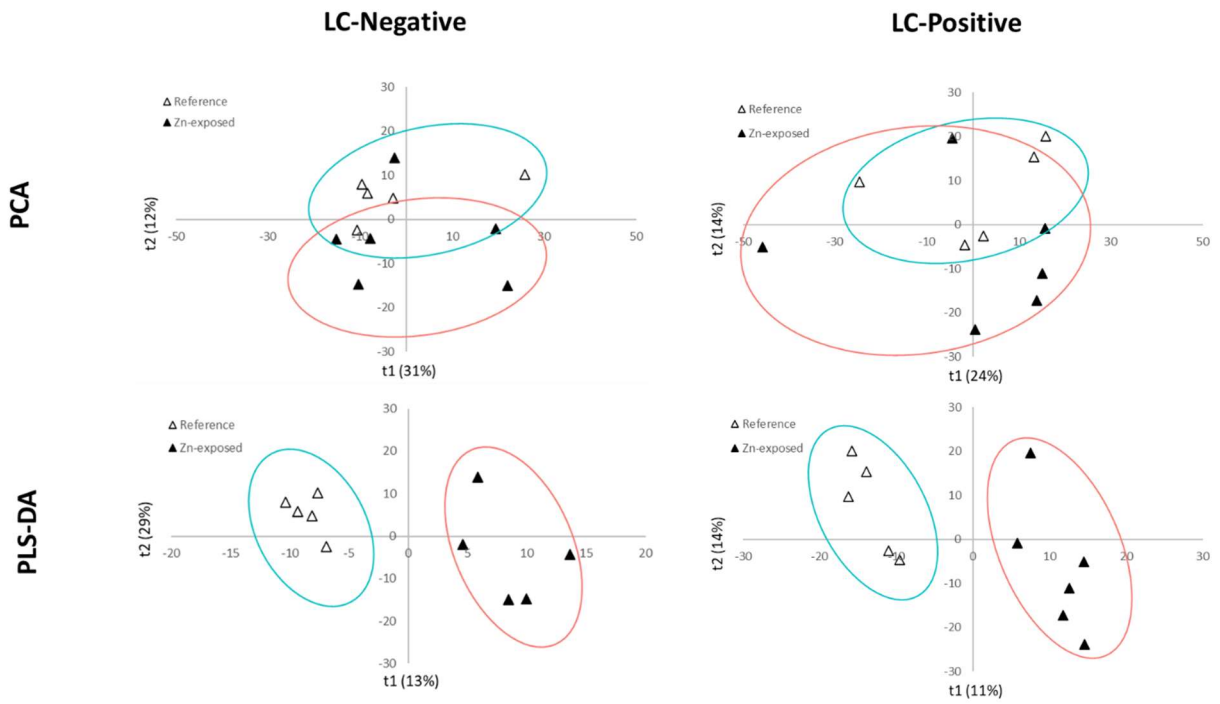
652

653 FIGURE CAPTIONS

654 Figure 1: Score plots of PCA and PLS-DA for negative mode (LC-Negative), positive mode (LC-Positive)  
655 of liquid chromatography. Ellipses score plots represented the confidence limit (95%) of Hotelling's T<sup>2</sup>  
656 statistic (Green ellipse for reference samples and red ellipse for Zn-Exposed samples).  
657

658 Figure 2: Box plots of the relative abundance of the 11 identified metabolites in *Mimachlamys varia* gills showing  
659 a significant difference between reference and Zn-exposed samples. Green plots represent the reference samples,  
660 red plots represent the zinc exposed samples. The mean value is given by the dark diamond-shaped symbol.  
661

662 Figure 1



663

664

665 Figure 2

666

667

668

669

670

671

672

673

674

675

676

677

678

679

680

681

682

683

684

685

686

687

688

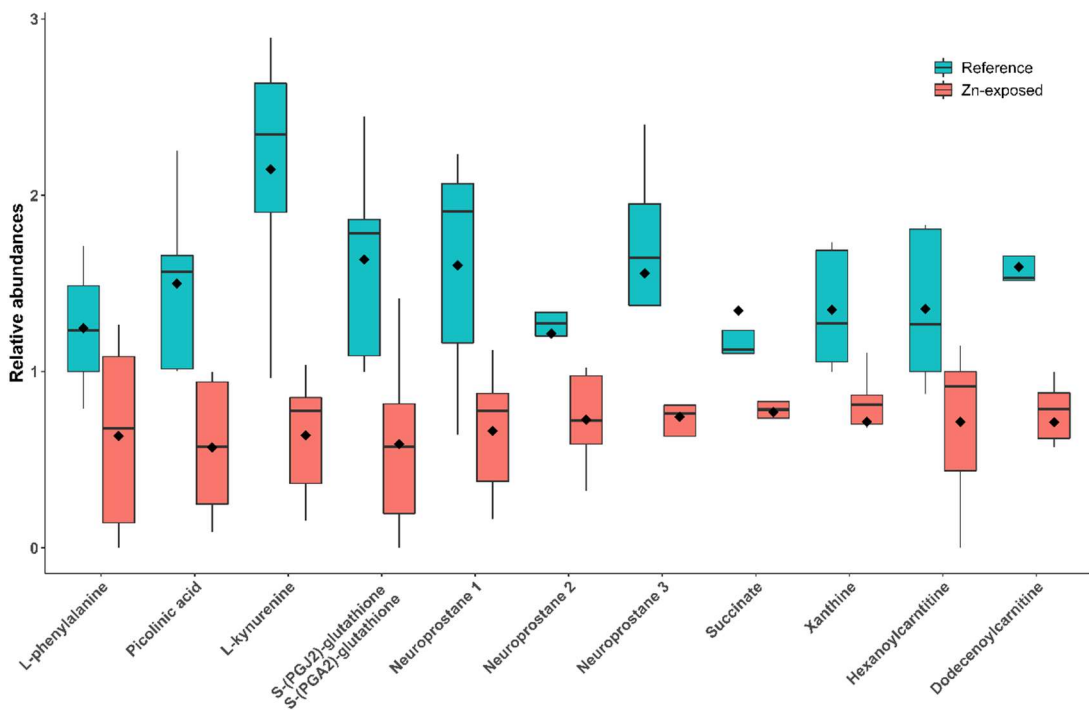
689

690

691

692

693



694  
695  
696  
697  
698  
699

Table 1: Identified metabolites varying after 48h-zinc exposure

Metabolite	Platform	Retention time (s)	Formula	Monoisotopic mass (Da)	Adduct	Observed mass (m/z)	Theoretical mass (m/z)	Mass error (ppm)	Ratio between reference and P-value exposed to Zn	
Picolinic acid	LC/MS Neg	198	C <sub>5</sub> H <sub>4</sub> N	123.032	[M-CO <sub>2</sub> -H] <sup>-</sup>	78.0346	78.0349	3.8	2.62	0.013
L-kynurenine	LC/MS Neg	417	C <sub>10</sub> H <sub>11</sub> N <sub>2</sub> O <sub>3</sub>	208.0848	[M-H] <sup>-</sup>	207.0770	207.0775	2.4	3.37	0.004
Neuroprostane 1	LC/MS Neg	678	C <sub>22</sub> H <sub>29</sub> O <sub>4</sub>	358.2144	[M-H] <sup>-</sup>	357.2066	357.2071	1.4	2.42	0.027
Neuroprostane 2	LC/MS Neg	601	C <sub>22</sub> H <sub>31</sub> O <sub>6</sub>	392.2199	[M-2H <sub>2</sub> O-H] <sup>-</sup>	391.2123	391.2126	0.8	1.67	0.050
Neuroprostane 3	LC/MS Neg	981	C <sub>22</sub> H <sub>31</sub> O <sub>5</sub>	376.225	[M-H <sub>2</sub> O-H] <sup>-</sup>	375.2167	375.2177	2.7	2.09	0.050
Succinate	LC/MS Neg	247	C <sub>4</sub> H <sub>5</sub> O <sub>4</sub>	118.0266	[M-H] <sup>-</sup>	117.0188	117.0193	4.3	1.75	0.050
L-phenylalanine	LC/MS Pos	417	C <sub>9</sub> H <sub>12</sub> NO <sub>2</sub>	165.079	[M+H] <sup>+</sup>	166.0869	166.0863	3.6	1.96	0.050
S-(PGA2)-glutathione S-(PGJ2)-glutathione	LC/MS Pos	658	C <sub>30</sub> H <sub>47</sub> N <sub>3</sub> O <sub>10</sub> SNa	641.2982	[M+Na] <sup>+</sup>	664.289	664.2874	2.4	2.78	0.001
Xanthine	LC/MS Pos	367	C <sub>5</sub> H <sub>5</sub> N <sub>4</sub> O <sub>2</sub>	152.0334	[M+H] <sup>+</sup>	153.0412	153.0407	3.3	1.89	0.018
Hexanoylcarnitine	LC/MS Pos	486	C <sub>13</sub> H <sub>26</sub> NO <sub>4</sub>	259.1784	[M+H] <sup>+</sup>	260.186	260.1856	1.5	1.90	0.044
Dodecenoylcarnitine	LC/MS Pos	562	C <sub>19</sub> H <sub>36</sub> NO <sub>4</sub>	341.2566	[M+H] <sup>+</sup>	342.2637	342.2639	0.6	2.23	<0.001

700  
701  
702  
703